

# Pervaporation of Aqueous Ethanol Solutions Through Pure and Composite Cellulose Membranes

ALI A. A. AL JANABI, OANA CRISTINA PARVULESCU\*, TANASE DOBRE, VIOLETA ALEXANDRA ION

University Politehnica of Bucharest, Chemical and Biochemical Engineering Department, 1-3 Gheorghe Polizu Str., 011061, Bucharest, Romania

*A procedure for synthesis of pure and composite membranes based on cellulose dissolved in NaOH-urea/thiourea solutions was developed. The phase inversion method was employed for cellulose solution conversion to supported and non-supported membranes. The use of tetraethyl orthosilicate (TEOS) as precursor in synthesis of composite cellulose membranes produced significant changes in their structure and pervaporation behaviour. The obtained membranes were tested for the pervaporation of ethanol-water system. Pervaporation performances, which were evaluated in terms of total permeate flux, separation factor and pervaporation separation index, strongly depended on TEOS loading, ethanol concentration and operation temperature.*

**Keywords:** alcohols dehydration, cellulose membrane, permeate flux, pervaporation, separation factor, swelling degree

Pervaporation (*p*ermeation + *e*vaporation) refers to the permeation of a liquid mixture through a membrane followed by species evaporation at the permeate side [1,2]. It is considered a feasible, economical and simple alternative to other methods (*e.g.*, distillation, solvent extraction), especially for separation of aqueous-organic systems. A classical example of aqueous-organic system separation via pervaporation is the alcohols dehydration [3-5]. The pervaporation is often coupled with chemical/biochemical reaction in order to control the reaction efficiency. The removal of water from esterification reactions [6], of ethanol from fermentation broths [7-8] or of acetone, butanol and ethanol (ABE) from their biosynthesis media [9-11] are the most known examples of coupled processes.

Pure and composite membranes based on polymer/biopolymer or zeolites are widely employed to separate aqueous-organic systems. The polymeric materials used as membrane precursors can be classified into three categories, *i.e.*, glassy, elastomeric (rubbery) and ionic. Generally, due to their highly controllable properties according to the cross-linking degree and counter-ions charging, the glassy and ionic polymers are more suitable for preparing water-selective membranes applied to dehydration, whereas the elastomeric ones are precursors of membranes used for removal of organic compounds from aqueous streams [12-14].

Repeat units characterizing the structure of some pure membranes widely employed for pervaporation of organics (hydrophobic membranes) or water (hydrophilic membranes) from organics-water mixture, especially from ethanol-water system, are shown in Fig. 1. In order to obtain very concentrated ethanol by pervaporation, pure and composite hydrophilic membranes based on polyvinyl alcohol [15-21], chitosan [22,23], sodium alginate [24-27], cellulose/bacterial cellulose [28-31] and zeolites [19,32-34] were successfully tested for water removal from ethanol-water mixture. On the other hand, relevant results have been reported concerning the removal of ethanol from dilute media via pervaporation using pure or composite

hydrophobic membranes based on various polymers, *e.g.*, polydimethylsiloxane, polytetrafluoroethylene, ethylene-propylene-diene terpolymer, polyurethane-urea, polyether block amide, poly(1-trimethylsilyl-1-propyne), natural or silicone rubber [35-38], as well as on zeolites [39].

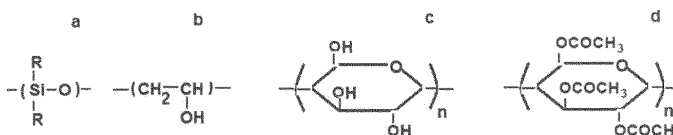


Fig. 1. Repeat units of some typical pervaporation membranes: (a) polydialkylsiloxane (hydrophobic), (b) polyvinyl alcohol (hydrophilic), (c) cellulose (hydrophilic), (d) cellulose triacetate (hydrophilic)

Pervaporation performances are usually evaluated in terms of membrane productivity and selectivity. Commonly, productivity is expressed as total or/and partial permeate flux and selectivity as separation factor. Pervaporation separation index, taking into account effects of both total permeate flux and separation factor, may be used to estimate the membrane ability of pervaporation separation [28,40].

Composite organic-inorganic membranes based on TEOS ( $\text{Si}(\text{OCH}_2\text{CH}_3)_4$ ) as an inorganic precursor have been widely applied to separate aqueous-organic systems [40,41]. Silanol groups ( $-\text{Si}-\text{OH}$ ) obtained by TEOS hydrolysis form siloxane bonds ( $-\text{Si}-\text{O}-\text{Si}-$ ) by dehydration reaction with other silanol groups or dealcoholysis reaction with ethoxy groups ( $-\text{Si}-\text{O}-\text{CH}_2\text{CH}_3$ ). For cellulose membranes, siloxane structures are dispersed among cellulose chains resulting in a more open network of hybrid membrane, *i.e.*, exhibiting a larger free-volume [41]. Hydrogen and covalent bonds can be formed between characteristic silanol groups of siloxane structures and  $-\text{OH}$  groups of cellulose, leading to a decrease in the flexibility of cellulose chains. Composite membranes may have a weakly or strongly hydrophilic character depending on the number of free and bonded silanol groups. Accordingly, if the free silanol groups are predominant, the

\*email: oana.parvulescu@yahoo.com; Tel.: (+40) 021 402 3810

membrane is strongly hydrophilic, otherwise it is weakly hydrophilic or even hydrophobic.

The present study has aimed at preparing and characterizing cellulose based membranes as well as at their testing for pervaporation separation of ethanol-water system. TEOS was used as an inorganic precursor in the synthesis of composite cellulose membranes. The effect of TEOS loading, ethanol concentration and operation temperature on pervaporation performances, expressed as total permeate flux, separation factor and pervaporation separation index, was evaluated.

## Experimental part

### Materials

Cotton cellulose powder (50 mm diameter, 0.600 g/cm<sup>3</sup> density), TEOS min 98 % as well as crystals of urea (C<sub>2</sub>H<sub>4</sub>N<sub>2</sub>O) and thiourea (C<sub>2</sub>H<sub>4</sub>N<sub>2</sub>S) were supplied by Sigma-Aldrich Chemie (Germany). NaOH pellets were purchased from Merck (Germany). All reagents were used without further purification. A paper support was used to prepare supported pure and composite membranes.

### Casting solution preparation

For the synthesis of pure cellulose membranes, a casting solution was prepared according to the following procedure: (i) an alkaline solution containing 9 wt. % NaOH and 5 wt. % urea/thiourea was selected as solvent for cellulose; (ii) cellulose powder was added to the alkaline solution forming a slurry with 8.5 wt. % cellulose, which was stirred for 3 hours at a temperature up to 30 °C; (iii) the stirred slurry was frozen at about -18 °C for 24 h; (iv) the frozen solution was thawed at room temperature and a hydrogel (casting solution) was obtained. For the synthesis of composite cellulose membranes, the casting solution prepared conforming to (i)-(iv) steps was mixed with TEOS for 10 min. Casting solutions with and without TEOS were prepared at 4 values of TEOS loading (0, 10, 30, 50%) expresses as TEOS mass percentage relative to the total mass of cellulose and TEOS.

### Membrane preparation

Supported and non-supported composite/pure cellulose membranes were synthesized by the phase-inversion method, as follows: (i) the casting solution with/without TEOS was spread as a thin film onto a glass plate (for non-supported membranes) or a paper support (for supported membranes) and then exposed to ambient air for 24 h; (ii) NaOH and urea/thiourea were removed from the film by treating with 1M HCl solution and rinsing with distilled water to a neutral pH; (iii) the rinsed membrane was kept in distilled water for 24 h and further dried at room temperature.

### Casting solution characterization

#### Optical Microscopy (OM)

Casting solutions with/without TEOS were analyzed by means of IOR ML-4M optical microscope (IOR, Romania).

#### Rheological tests

Dynamic viscosity of casting solution with/without TEOS was estimated based on rheological measurements performed using a Rheotest 2 rotary viscosimeter (MLW, Germany) equipped with coaxial cylinders.

### Non-supported membrane characterization

#### Scanning Electron Microscopy (SEM)

Surface morphology of pure and composite non-supported cellulose membranes was examined by an

AURIGA scanning electron microscope (Carl Zeiss, Germany) operated at 25 kV. The samples were gold coated prior to SEM analysis.

### X-ray diffraction (XRD)

XRD patterns of non-supported cellulose based membranes were obtained with a D/Max-2550 PC X-ray diffractometer (Rigaku, Japan) using Cu K $\alpha$  radiation, operation voltage of 40 kV and current of 300 mA.

### Supported membrane testing

#### Swelling tests

Supported membrane swelling caused by the sorption of liquids was determined based on a gravimetric procedure. Swelling degree of a membrane, *SD*, was calculated using eq. (1), where *m<sub>e</sub>* is the equilibrium mass of swollen membrane and *m<sub>0</sub>* the mass of dry membrane. The mass of dry membrane was obtained by drying a membrane sample in an oven at 70 °C for 9 h. The dry sample was then put in 30 cm<sup>3</sup> of ethanol-water solution and kept for 48 h until the equilibrium state was reached. The samples were weighed using a Kern ABS-N analytical balance (Kern & Sohn, Germany) with an accuracy of 0.0001 g.

$$DS = \frac{(m_e - m_0)}{m_0} \times 100 \quad (1)$$

#### Pervaporation tests

Pervaporation experiments were carried out in a batch stirred cell operated under vacuum. The supported membrane was put on a sintered steel disk, 5  $\mu$ m average pore diameter, welded to the top of the lower compartment. The upper compartment containing the feed ethanol-water mixture was closed in order to stop any loss from feed. Before starting an experiment, the membrane was equilibrated for 30 min with a liquid mixture of the same composition as that of the feed. The swollen membrane was then placed in the pervaporation device and the feed liquid was charged to the upper compartment, wherein a magnetic stirring was used to mix the ethanol-water solution. This stirring aimed at minimizing the mass transfer resistance between the feed liquid and membrane. A vacuum of 100 mbar was applied to the lower compartment by means of a vacuum pump (Sartorius, Japan) and the permeate was collected in an ice trap.

The liquid temperature in the feed compartment and the system mass were measured before starting (*t<sub>i</sub>*, *m<sub>i</sub>*) and after finishing (*t<sub>f</sub>*, *m<sub>f</sub>*) an experiment. Total pervaporation flux, *J<sub>p</sub>*, was estimated using eq. (2), where *m* is the mass of the permeate collected during the pervaporation time,  $\Delta\tau$ , and *A* the effective membrane area.

$$J_p = \frac{m}{A\Delta\tau} = \frac{m_i - m_f}{A\Delta\tau} \quad (2)$$

Ethanol concentrations in the permeate and feed samples were estimated using an Atago Abbe refractometer (Atago, Japan). Separation factor relative to water and ethanol,  $\alpha_{w/eth}$ , was calculated with eq. (3), where *X* and *Y* represent the mass fractions of species in the feed and permeate, respectively.

$$\alpha_{w/eth} = \frac{(Y_w / Y_{eth})}{(X_w / X_{eth})} \quad (3)$$

Pervaporation separation index, *PSI*, was determined depending on *J<sub>p</sub>* and  $\alpha_{w/eth}$  with eq. (4).

$$PSI = J_p (\alpha_{w/eth} - 1) \quad (4)$$

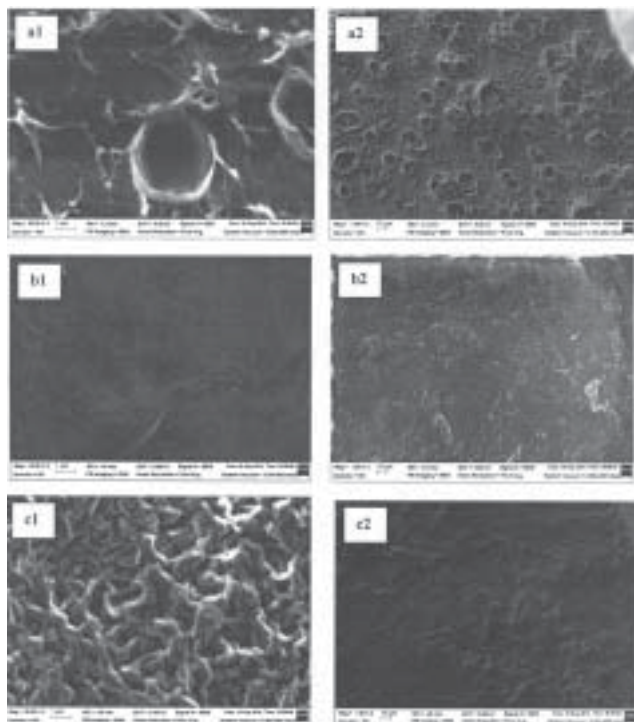


Fig. 2. SEM images of pure and composite membranes prepared from a casting solution with: (a) urea; (b) thiourea; (c) thiourea and 10 % TEOS; (1) 1  $\mu\text{m}$  scale bar; (2) 10  $\mu\text{m}$  scale bar.

## Results and discussions

### SEM measurements

Representative SEM micrographs illustrating the surface morphology of pure and composite cellulose membranes are shown in figure 2. A pure cellulose membrane (PC) prepared by dissolving the cellulose in urea alkaline solution exhibits a non-homogenous surface with large (10-20  $\mu\text{m}$  diameter) and small (1-2  $\mu\text{m}$  diameter) concavities (fig. 1a). These concavities, covering more than 50 % from total surface, are caused by an incomplete cellulose dissolution. A PC membrane synthesized using thiourea instead of urea has a very homogenous and dense surface (fig. 1b), probably due to a higher dissolution power of thiourea alkaline solution. A composite cellulose membrane obtained from a casting solution with thiourea and 10 % TEOS (10CC) presents a more open network (fig. 1c), as effect of siloxane structures dispersed among cellulose chains. Casting solutions with thiourea were further analyzed and used to prepare pure and composite membranes.

### XRD measurements

XRD analysis for PC and 10CC membranes aimed at obtaining quantitative data on their crystallinity. Results presented in figure 3 and table 1 for dry membranes emphasize that 10CC membrane has a crystallinity larger than that of PC, *i.e.*, 73.5 % *vs.* 53 %. These values are lower than those of dry bacterial cellulose membranes (usually over 95% [42]), which were successfully tested for pervaporation separation of ethanol-water system [28].

### OM measurements

Sample	Minimum-maximum crystallinity		% Crystalline	% Amorphous	Global area	Reduced area
3 (PC)	5.000	54.387	53.0	47.0	159.6	84.61
5 (10CC)	5.000	74.875	73.5	26.5	236.8	174.2

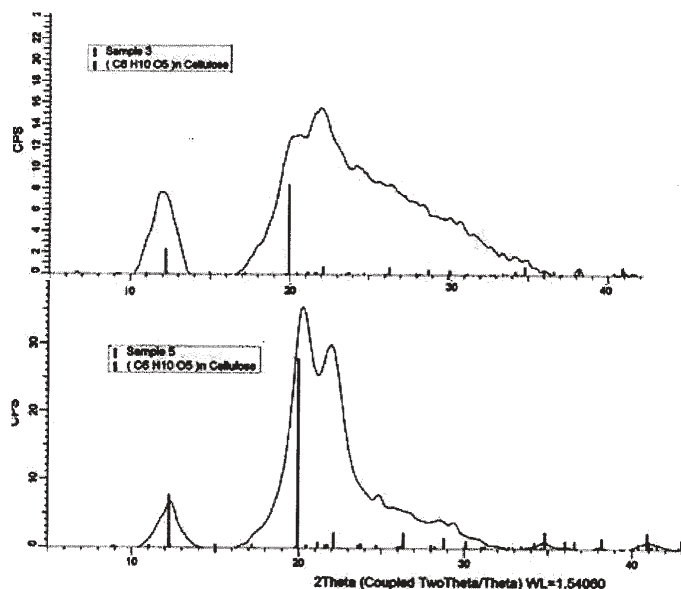


Fig. 3. XRD pattern of pure (sample 3) and 10 % TEOS composite (sample 5) cellulose membranes.

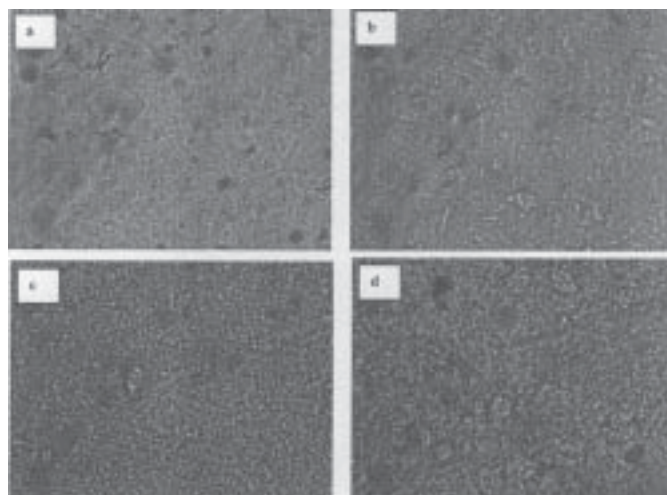


Fig 4. OM images (50x magnification) of casting solutions with and without TEOS: (a) without TEOS; (b) 10 % TEOS; (c) 30 % TEOS; (d) 50 % TEOS.

OM images of casting solutions with and without TEOS which are shown in figure 4 indicate the appearance of some local microstructures depending on TEOS content. It seems that an increase in TEOS loading led to an increase in solution dynamic viscosity.

### Rheological measurements

Rheological tests of casting solutions with and without TEOS were conducted at two values of operation temperature (25 and 40  $^{\circ}\text{C}$ ), four levels of TEOS loading (0-50 %) and a shear rate ranging from 0.5 to 122  $\text{s}^{-1}$ .

Plots in figure 5, describing the variation of shear stress,  $\tau$  (Pa), depending on shear rate,  $\dot{\gamma}$  ( $\text{s}^{-1}$ ), emphasize the following aspects: (i) for pure cellulose and 10 % TEOS casting solution at 25  $^{\circ}\text{C}$ , the dependency between  $\tau$  and  $\dot{\gamma}$  is linear (eq. (5)) and the intercept ( $\eta_0$ ) is about 0 Pa, corresponding to a newtonian fluid whose dynamic viscosity is equal to the line slope ( $\eta$ ); data presented in figure 5 and table 2 highlight similar values of viscosity, *i.e.*, 0.476  $\text{Pa}\cdot\text{s}$  and 0.518  $\text{Pa}\cdot\text{s}$ , respectively; (ii) for pure

Table 1  
XRD ANALYSIS RESULTS

cellulose solution at 40 °C, the dependency between  $\tau$  and  $\gamma$  is linear (eq. (5)) with the slope  $\eta = 0.462 \text{ Pa}\cdot\text{s}$  and the intercept  $\tau_0 = 7.422 \text{ Pa}$ , corresponding to a Bingham plastic fluid with a dynamic viscosity of  $0.462 \text{ Pa}\cdot\text{s}$  and a yield stress of  $7.422 \text{ Pa}$ ; (iii) for the other experiments,  $\tau$  varies with  $\gamma$  according to a power law, *i.e.*, Ostwald de Waele relationship (eq. (6)), where  $K (\text{Pa}\cdot\text{s}^n)$  is the flow consistency index and  $n$  the flow behaviour index; results shown in figure 5 emphasize a characteristic behaviour of pseudoplastic fluid characterized by  $n < 1$ , whose apparent viscosity,  $\eta_{app} (\text{Pa}\cdot\text{s})$ , was calculated depending on  $\gamma$  using eq. (7); curves depicted in figure 5 and data summarized in table 2 reveal a decreasing variation between  $\eta_{app}$  and  $\gamma$  as well as an increase in  $\eta_{app}$  with temperature and TEOS mass loading.

$$\tau = \eta\gamma + \tau_0 \quad (5)$$

$$\tau = K\gamma^n \quad (6)$$

$$\eta_{app} = K\gamma^{n-1} \quad (7)$$

### Swelling tests

Because there is a strong dependence between the pervaporation performances and membrane swelling, the establishment of the effect of operational parameters on the swelling degree,  $SD$ , is an important issue. Swelling

experiments were conducted at 7 values of water mass percentage in the feed,  $c_w$  (17.2-80.6 %), 4 values of TEOS mass loading,  $c_{TEOS}$  (0-50 %) and 2 values of operation temperature,  $t$  (25 °C and 40 °C). Results presented in table 3 and figure 6 show the variation of  $SD$  with operational parameters.

Excepting the membrane with the highest TEOS loading ( $c_{TEOS} = 50 \%$ ), it is noticed an increase in  $SD$  with  $c_w$  and  $c_{TEOS}$ . Increasing variation of  $SD$  with  $c_w$  might be an effect of a larger number of water molecules at the feed side, of a small size of water molecule, as well as of a hydrophilic character of cellulose based membranes resulting in strong interactions between water molecules and reactive -OH groups of membrane matrix. Data depicted in figure 6 highlight that  $SD$  varies more sharply with the feed water content for pure cellulose membrane, possibly owing to its more flexible cellulose chains. Moreover,  $SD$  increases with TEOS loading, especially for low water concentrations ( $c_w = 17.2-38.4 \%$ ), mainly due to a more open network of dry hybrid membrane. The membrane containing 50 % TEOS has an atypical behaviour, *i.e.*,  $SD$  is almost constant (*cca.* 54 %) for  $c_w = 23.8-64.1 \%$ . This might be a consequence of a significant loss in the flexibility of cellulose chains due to the hydrogen and covalent bonds formed between silanol groups of siloxane structures and -OH groups of cellulose chains. Data summarized in table 3 highlight a slow increase (up to 10 %) in  $SD$  with the operation temperature for all membrane types, possibly

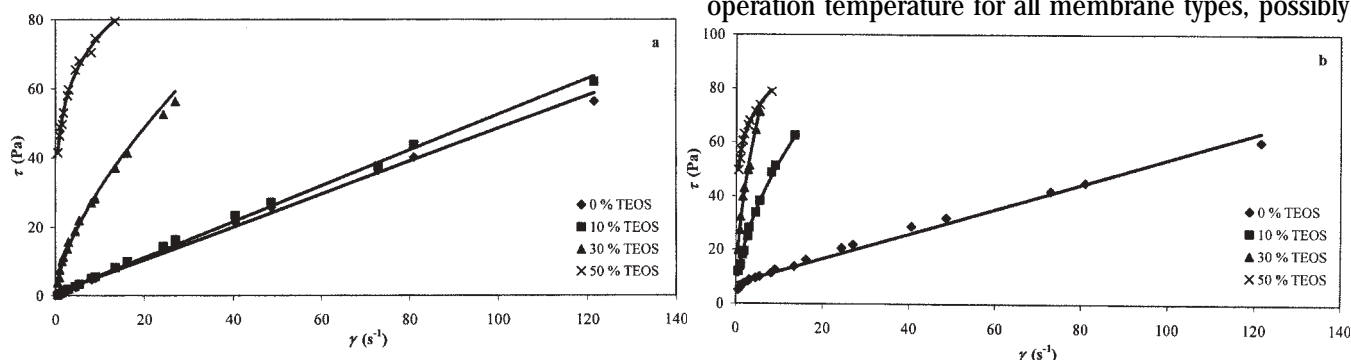


Fig. 5. Shear stress,  $\tau$ , vs. shear rate,  $\gamma$ , at 25 °C (a) and 40 °C (b) for casting solutions with and without TEOS.

Temperature °C	TEOS mass loading %	Constants in Eqs. (5)-(7)	Fluid type	Dynamic viscosity Pa·s
25	0	$\eta=0.476 \text{ Pa}\cdot\text{s}$ , $\tau_0=0.892 \text{ Pa}$	Newtonian	0.476
	10	$\eta=0.518 \text{ Pa}\cdot\text{s}$ , $\tau_0=0.780 \text{ Pa}$	Newtonian	0.518
	30	$K=6.897 \text{ Pa}\cdot\text{s}^n$ , $n=0.652$	Pseudoplastic	2.19-8.78
	50	$K=47.541 \text{ Pa}\cdot\text{s}^n$ , $n=0.200$	Pseudoplastic	5.92-82.78
40	0	$\eta=0.462 \text{ Pa}\cdot\text{s}$ , $\tau_0=7.422 \text{ Pa}$	Bingham plastic	0.462
	10	$K=15.130 \text{ Pa}\cdot\text{s}^n$ , $n=0.543$	Pseudoplastic	4.60-20.77
	30	$K=30.172 \text{ Pa}\cdot\text{s}^n$ , $n=0.517$	Pseudoplastic	13.36-42.17
	50	$K=56.151 \text{ Pa}\cdot\text{s}^n$ , $n=0.164$	Pseudoplastic	9.77-100.23

**Table 2**  
DYNAMIC VISCOSITY OF CASTING SOLUTIONS DEPENDING ON PROCESS PARAMETERS

**Table 3**  
DEPENDENCE OF SWELLING DEGREE (%) ON WATER MASS PERCENTAGE IN THE FEED,  $c_w$ , TEOS MASS LOADING AND OPERATION TEMPERATURE

$c_w$ %	0 % TEOS		10 % TEOS		30 % TEOS		50 % TEOS	
	25 °C	40 °C	25 °C	40 °C	25 °C	40 °C	25 °C	40 °C
17.2	17.55	19.35	36.48	37.53	39.32	41.3	43.28	45.28
23.8	24.05	25.05	42.98	44.05	49.41	50.62	52.54	53.54
38.4	43.14	44.14	49.81	51.38	56.3	57.5	53.57	54.17
58.1	54.59	56.59	55.35	55.31	61.75	63.24	53.6	53.62
64.1	58.86	59.86	61.13	62.37	65.12	66.35	53.72	53.72
71.4	63.59	64.59	63.88	65.97	67.33	68.55	55.71	55.71
80.6	72.46	73.16	67.31	68.35	69.06	70.94	64.32	64.32

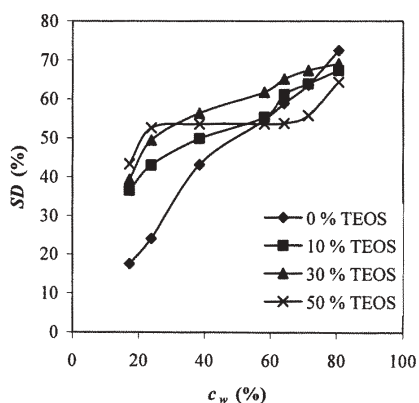


Fig. 6. Swelling degree,  $SD$ , vs. water mass percentage in the feed,  $c_w$ , at 25 °C and various values of TEOS mass loading

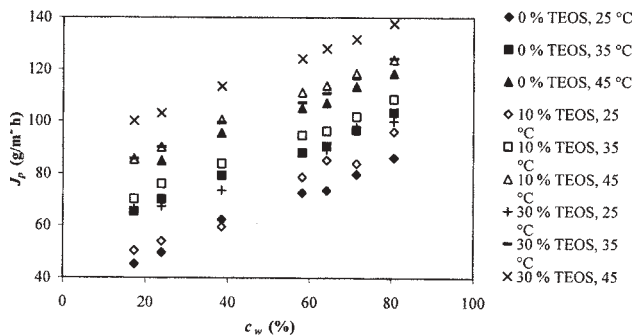


Fig. 7. Total pervaporation flux,  $J_p$ , vs. water mass percentage in the feed,  $c_w$ , at various values of TEOS mass loading and pervaporation temperature

caused by an enhancement of plasticization effect at higher temperatures.

#### Pervaporation tests

Pervaporation performances have been expressed in terms of total permeate flux,  $J_p$ , separation factor,  $\alpha_{w/eth}$  and pervaporation separation index,  $PSI$ . Experiments were performed at 7 values of water mass percentage in the feed,  $c_w$  (17.2-80.6 %), 3 values of TEOS mass loading,  $c_{TEOS}$  (0-30 %) and 3 values of operation temperature,  $t$  (25-45°C).

Results presented in figure 7 emphasize an increase in  $J_p$  with all operational parameters. According to data summarized in table 3, an increase in each parameter determined an increase in  $SD$ , resulting in an enhancement of molecular diffusion of permeate species. Moreover, higher temperatures determined larger values of species diffusion coefficient.

The dependence between  $J_p$  and  $t$  was expressed by Arrhenius equation (eq. (8)), where  $J_p$  is the permeation rate constant,  $E_p$  the activation energy of the process,  $R$  the gas constant and  $T$  the absolute temperature. Values of  $E_p$  and  $J_{p0}$  which were estimated based on experimental data ( $J_p$  vs.  $1/T$ ) under various operation conditions, are summarized in table 4. Characteristic values of  $E_p$  are in a good agreement with those reported by other researchers [40,43,44]. Statistical analysis of tabulated data led to eq. (9) expressing the dependency between activation energy and operational parameters, i.e., water mass fraction in the feed,  $\omega_w$ , and TEOS mass fraction,  $\omega_{TEOS}$ . A root mean square error of 1.74 relative to experimental ( $E_p$ ) and calculated ( $E_{p,c}$ ) values of activation energy (fig. 8) was obtained.

The effect of operational parameters on separation factor,  $\alpha_{w/eth}$  is shown in figure 9. It is observed that  $\alpha_{w/eth}$  is strongly dependent on  $c_w$  and  $c_{TEOS}$ . For PC membrane  $\alpha_{w/eth}$  drops from 11.9-13.5 to 4.2-5.1, for 10CC membrane from 10.5-11.5 to 3.5-4.7, whereas for 30CC it increases from about 1.1 to 1.8-2.6. Accordingly, for PC and 10CC membranes,  $\alpha_{w/eth}$  decreases as  $c_w$  and  $c_{TEOS}$  increase, whereas for 30CC membrane,  $\alpha_{w/eth}$  increases as  $c_w$  increases and  $c_{TEOS}$  decreases. This behaviour suggests that 10CC membrane is strongly hydrophilic and 30CC membrane has a weakly hydrophilic character. Consequently, the following configurations can be assumed for the composite cellulose membranes (fig. 10): (i) 10CC membrane contains siloxane structures with low molecular mass whose silanol groups are rather free than bonded by -OH groups belonging to cellulose chains, leading to a hydrophilicity similar or higher than that of pure cellulose and a lower chain flexibility; (ii) on the contrary, 30CC membrane includes siloxane structures with higher molecular mass and silanol groups which are predominately bonded by -OH groups of cellulose chains, resulting in a structure with weak hydrophilicity and less

Table 4

THE EFFECT OF WATER MASS PERCENTAGE IN THE FEED,  $c_w$ , AND TEOS MASS LOADING ON ACTIVATION ENERGY,  $E_p$ , AND PERMEATION RATE CONSTANT,  $J_{p0}$

$c_w$ %	0 % TEOS		10 % TEOS		30 % TEOS	
	$E_p$ kJ/mol	$J_{p0}$ kg/(m <sup>2</sup> .h)	$E_p$ kJ/mol	$J_{p0}$ kg/(m <sup>2</sup> .h)	$E_p$ kJ/mol	$J_{p0}$ kg/(m <sup>2</sup> .h)
17.2	25.2	1213	20.8	232.6	16.1	45.6
23.8	21.2	267.2	20.3	200.7	16.8	60.8
38.4	16.8	56.3	20.7	164.2	17.1	75.9
58.1	14.6	25.9	13.6	18.9	13.5	21.4
64.1	14.7	28.9	11.4	8.34	14.2	28.2
71.4	13.8	21.8	13.6	20.5	11.8	11.3
80.6	12.6	14.2	9.9	5.5	12.6	16.5

flexible chains. For both more hydrophilic membranes, an increase in  $c_w$  determines an enhancement of membrane swelling which has a negative influence on  $\alpha_{w/eth}$ , this unfavourable effect being more important for 10CC membrane which exhibits a higher swelling. Accordingly, the swollen hydrophilic membrane allows some ethanol molecules to penetrate and to diffuse together with water molecules through the membrane determining a decrease in  $\alpha_{w/eth}$ . On the other hand, for 30CC less hydrophilic membrane, an increase in  $SD$  with  $c_w$  leads to an increase in  $\alpha_{w/eth}$ . However, conforming to data shown in figure 8, characteristic values of  $\alpha_{w/eth}$  for 30CC membrane are less than those of PC and 10CC hydrophilic membranes.

$$J_p = J_{p0} \exp\left(\frac{-E_p}{RT}\right) \quad (8)$$

$$E_{p,c} = 24.5 - 14.8\omega_w - 16.3\omega_{TEOS} + 26.1\omega_{TEOS}^2 \quad (9)$$

For PC and 10 CC membranes, results presented in figures 6, 7 and 9 reveal that an increase in  $SD$  has an

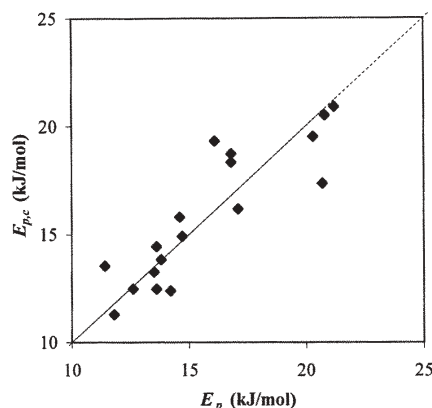


Fig. 8. Parity diagram between experimental ( $E_p$ ) and calculated ( $E_{p,c}$ ) values of activation energy

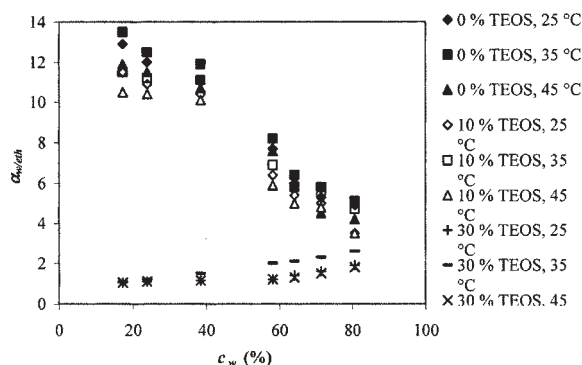


Fig. 9. Separation factor,  $\alpha_{w/eth}$  vs. water mass percentage in the feed,  $c_w$ , at various values of TEOS mass loading and pervaporation temperature.

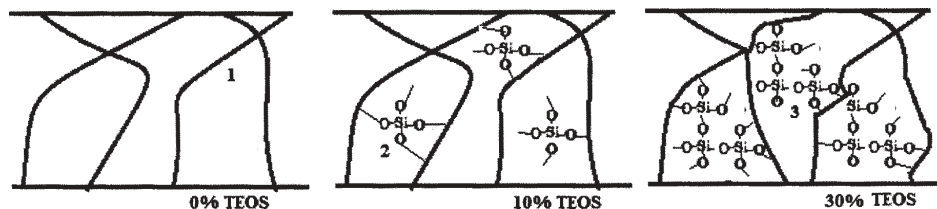


Fig. 10. Possible structures of pure and composite cellulose membranes

No.	Membrane type	Operation conditions (liquid system, $c_w$ , $t$ )	Activation energy kJ/mol	Total permeate flux $\text{kg}/(\text{m}^2 \cdot \text{h})$	Separation factor	Reference
1	Polyvinyl alcohol-TEOS	Dioxane-water, 10-90 %	30-50	0.7-2	10-1000	[40]
2	Sodium carboxymetil cellulose-TEOS	Ethanol-water	-	0.00005-0.007	400-4000	[41]
3	Polyacrylonitrile	Ethanol-water, 70 °C	35	0.042	12500	[43]
4	Polyvinyl alcohol	Ethanol-water, 70 °C	-	0.38	140	[43]
5	Acylonitril-acrylic acid copolymer,	Ethanol-water, 80 %	35-65	0.047-0.12	70-200	[44]
6	Polyeter uretanes	Ethanol-water, 50 %	-	0.06-0.4	2-18	[45]
7	Cellulose acetate	Ethanol-water, 50 %	-	0.5-1.2	2-4	[46]
8	Polysulphone	Ethanol-water, 50 %	-	0.003-0.006	332	[46]
9	Chitosan-fibroin	Ethanol-water, 5-70 %	-	0.065-0.45	10-400	[47]
10	Cellulose	Ethanol-water 17.2-80.6 %	12.6-25.2	0.044 – 0.118	3.8-13.3	This paper
11	Cellulose-10% TEOS	Ethanol-water 17.2-80.6 %	9.9-20.8	0.048 – 0.130	2.8-11.6	This paper

**Table 5**  
PERFORMANCES OF LIQUID MIXTURE PERVAPORATION USING HYDROPHILIC MEMBRANES

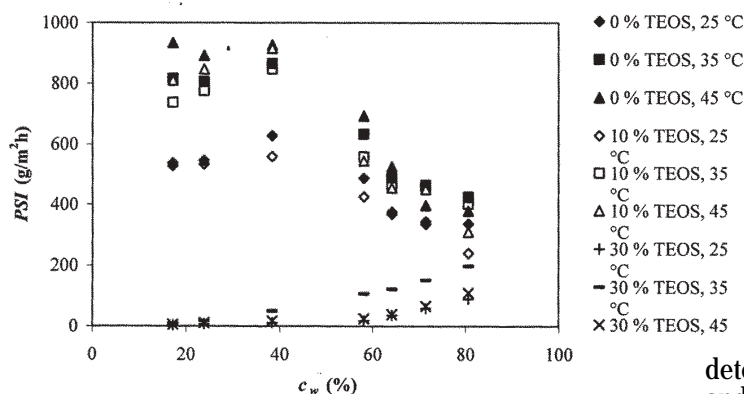


Fig. 11. Pervaporation separation index,  $PSI$ , vs. water mass percentage in the feed,  $c_w$ , at various values of TEOS mass loading and pervaporation temperature.

favourable effect on  $J_p$  as well as an unfavourable one on  $\alpha_{w/eth}$ . Accordingly, for operation of PC and 10 CC membranes under experimental conditions considered in this study ( $c_w = 17.2-80.6\%$ ,  $t = 25-45\text{ °C}$ ), an increase in  $SD$  from about 18 to 73 % has produced an increase in  $J_p$  from 45.2 to 123.9  $\text{g}/(\text{m}^2 \times \text{h})$  and a decrease in  $\alpha_{w/eth}$  from 13.5 to 3.5, respectively. These data are compared in Table 5 with results reported in the literature, which present the same opposite variation trend of  $J_p$  and  $\alpha_{w/eth}$  [40,41,43-47].

In order to select membranes with maximum performances related to both  $J_p$  and  $\alpha_{w/eth}$ , a pervaporation separation index,  $PSI$  was estimated with eq. (4). The dependency of  $PSI$  on operational parameters illustrated in figure 11 reveals that: (i) 30 CC membrane has the lowest  $PSI$  (up to 200  $\text{g}/(\text{m}^2 \times \text{h})$ ); (ii) PC and 10 CC membranes operated at 35 and 45 °C have almost similar values of  $PSI$  (from 310 to 934  $\text{g}/(\text{m}^2 \times \text{h})$ ) and the highest values of  $PSI$ , i.e., from 738 to 934  $\text{g}/(\text{m}^2 \times \text{h})$ , correspond to  $c_w = 17.2-38.4\%$ . According to results presented in tables 6 and 8 related to PC and 10 CC membranes operated at 35°C and 45°C, an increase in  $c_w$  from 17.2 to 38.4 %

determines an increase in  $J_p$  from 65.3 to 100.6  $\text{g}/(\text{m}^2 \times \text{h})$  and a decrease in  $\alpha_{w/eth}$  from 13.5 to 10.1, respectively.

## Conclusions

Cellulose based membranes were synthesized, characterized and tested in pervaporation of water-ethanol mixtures. Pure cellulose membranes were prepared by phase inversion procedure starting from a casting solution resulted from cellulose dissolving in urea or thiourea alkaline media. Experimental attempts proved that cellulose dissolution was improved in the presence of thiourea. Composite membranes were obtained based on a casting solution wherein TEOS was added. Characteristic SEM and XRD measurements of obtained membranes highlighted that these are similar to other membranes commonly used for pervaporation of ethanol-water system.

Swelling and pervaporation tests of pure and composite cellulose membranes were performed under various operation conditions. The effect of operational parameters (water mass percentage in the feed,  $c_w = 17.2-80.6\%$ , TEOS mass loading,  $c_{TEOS} = 0-50\%$ , and operation temperature,  $t = 25-45\text{ °C}$ ) on swelling degree,  $SD$ , and pervaporation performances (total permeate flux,  $J_p$ , separation factor,  $\alpha_{w/eth}$  and pervaporation separation index,  $PSI$ ) was studied. Experimental results revealed an increase in  $SD$  and  $J_p$  with all operational parameters. The

dependence between  $J_p$  and  $t$  was expressed by Arrhenius equation and values of activation energy ranging between 9.9 and 25.2 kJ/mol were obtained, conforming to results reported in the literature. An empirical correlation linking the activation energy to feed water concentration and TEOS loading was obtained by statistical analysis.

For pure cellulose (PC) membrane and 10 % TEOS composite cellulose membrane (10CC), an increasing variation of  $SD$  with  $c_w$  and  $t$  was obtained. Moreover, an increase in  $SD$  from about 18 to 73 % determined an increase in  $J$  from 45.2 to 123.9 g/(m<sup>2</sup>×h) and a decrease in  $\alpha_{w/eth}$  from 13.5 to 3.5, respectively. The highest values of PSI, i.e., from 738 to 934 g/(m<sup>2</sup>×h), were obtained for dehydration of ethanol solutions containing 17.2-38.4 % water via pervaporation through PC and 10 CC strongly hydrophilic membranes at 35 °C and 45 °C. On the contrary, 30CC weakly hydrophilic membrane had the lowest values of PSI (up to 200 g/(m<sup>2</sup>×h)) and  $\alpha_{w/eth}$  (up to 2.5). These results emphasize that PC and 10 CC membranes might be successfully applied to dehydrate ethanol solutions over 60 wt% at temperatures larger than 35 °C.

*Acknowledgements:* Ali A. A. AL JANABI expresses his gratitude to the Iraqi Ministry of Higher Education and Scientific Research as well as to the Al-Furat Al-Awsat Technical University for their funding. Violeta A. ION is grateful to Sectorial Operational Program Human Resources Development (SOP HRD), financed from the European Social Fund and the Romanian Government under the contract number POSDRU/159/1.5/S/137390, for financial support. The authors thank to Mariana BUC'OIU, Rodica ANGHEL and Monica MARE' for experimental assistance and to Cristian SIMION for comments that greatly improved the manuscript.

## References

- NEEL J., Introduction to Pervaporation, in: Pervaporation Membrane Separation Processes, Huang R. Y. M. (Ed.), Elsevier, Amsterdam, 1991.
- NOBLE D.R., STERN A.S., Membrane Separation Technology, Elsevier, Amsterdam, 1995.
- SANDERS U., SOUKUP P., J. Membr. Sci., **36**, 1988, p. 463.
- JAIMES J.H.B., ALVAREZ M.E.T., ROJAS J.V., FILHO R.M., Chem. Eng. Trans., **38**, 2014, p. 139.
- PAKKETHATIK., BOONMALERT A., CHAISUWAN T., WONGKASEMJIT S., Desalination, **267**, 2011, p. 73.
- STEINIGEWEG S., GMEHLING J., Chem. Eng. Process., **43**, 2004, p. 447.
- O'BRIEN J.D., CRAIG C.J.Jr., Appl. Microbiol. Biotechnol., **44**, 1996, p. 699.
- JAIN A., CHAURASIA S.P., J. Environ. Res. Dev., **4**, no. 4, 2014, p. 387.
- DONG Z., LIU G., LIU S., LIU Z., JIN W., J. Membr. Sci., **450**, 2014, p. 38.
- SETLHAKU M., HEITMANN S., GORAK A., WICHMANN R., Bioresour. Technol., **136**, 2013, p. 102.
- ALJANABI A.A.A., DOBRE T., PARVULESCU O.C., DANCUI D.T., PATRICHI C., Rev. Chim. (Bucharest), **66**, no. 12, 2015, p. 2070
- MAIOR I., ALBU A.M., GABOR R., Appl. Mech. and Mat., **760**, 2015, p. 245.
- SHAH D., KISSICK K., GHORPADE A., HANNAH R., BHATTACHARYYA D., J. Membr. Sci., **179**, 2000, p. 185.
- VANE L.M., J. Chem. Technol. Biotechnol., **80**, 2005, p. 603.

- AMNUAYPANICH S., PATTHANA J., PHINYOCHEEP P., Chem. Eng. Sci., **64**, 2009, p. 4908.
- LI B.B., XU Z.L., QUSAY F.A., LI R., Desalination, **193**, 2006, p. 171.
- BOLTO B., TRAN T., HOANG M., XIE Z., Prog. Polym. Sci., **34**, 2009, p. 969.
- GIMENES L.M., LIU L., FENG X., J. Membr. Sci., **295**, 2007, p. 71.
- SHAH D.S., Pervaporation of solvent mixtures using polymeric and zeolitic membranes: Separation studies and modelling, Ph.D. Thesis, University of Kentucky, 2001.
- ZHANG Q.G., LIU Q.L., JIANG Z.Y., CHEN Y., J. Membr. Sci., **287**, 2007, p. 237.
- ZHOU K., ZHANG Q.G., HAN G.L., ZHU A.M., LIU Q.L., J. Membr. Sci., **448**, 2013, p. 93.
- AKIRA M., YOSHIO S., HISASHI O., SHUZO Y., J. Appl. Polym. Sci., **37**, no. 12, 1989, p. 3375.
- SUNITHA K., SATYANARAYANA S.V., SRIDHAR S., Carbohydr. Polym., **87**, no. 2, 2012, p. 1569.
- BHAT S.D., AMINABHAVI T.M., Sep. Purif. Rev., **36**, 2007, p. 203
- KALYANI S., SMITHA B., SRIDHAR S., KRISHNAIAH A., Desalination, **229**, 2008, p. 68.
- MAGALAD V.T., SUPALE A.R., MARADUR S.P., GOKAVI G.S., AMINABHAVI T.M., Chem. Eng. J., **159**, 2010, p. 75.
- YEOM C.K., LEE K.H., J. Appl. Polym. Sci., **69**, 1998, p. 1607.
- DUBEY V., CHHAYA S., SINGH L., RAMANA K.V., CHAUHAN R.S., Sep. Purif. Technol., **27**, no. 1, 2002, p. 163.
- JIRARATANANON R., CHANACHAI A., HUANG R.Y.M., UTTAPAP D., J. Membr. Sci., **195**, 2002, p. 143.
- KAWEKANNETRA P., CHUTINATE N., MOONAMART S., KAMSAN T., CHIU T.Y., Desalination, **271**, 2011, p. 88.
- SHENG J., MORA J.C., Desalination, **80**, no. 1, 1991, p. 71.
- AHN H., LEE H., LEE S.B., LEE Y., Desalination, **193**, 2006, p. 244.
- KITA H., CHEN X., LIN X., OKAMOTO K., YAMAMURA T., ABE J., Fuel Chem. Div. Preprints, **48**, no. 1, 2003, p. 489.
- KUNNAKORN D., RIRKSOMBOON T., AUNGKAVATTANA P., KUANCHERTCHOOR N., ATONG D., KULPRATHIPANJA S., WONGKASEMJIT S., Desalination, **269**, 2011, p. 78.
- SUKITPANEENT P., CHUNG T.S., JIANG L.Y., J. Membr. Sci., **362**, 2010, p. 393.
- ZHOU H., SHI R., JIN W., Sep. Purif. Technol., **127**, 2014, p. 61.
- LE N.L., WANG Y., CHUNG T.S., J. Membr. Sci., **379**, 2011, p. 174.
- SMULEAC V., WU J., NEMSER S., MAJUMDAR S., BHATTACHARYYA D., J. Membr. Sci., **352**, 2010, p. 41.
- WEYD M., RICHTER H., PUHLFURS P., VOIGT I., HAMEL C., SEIDEL-MORGENSTERN A., J. Membr. Sci., **307**, 2008, p. 239.
- KITTUR A.A., JEEVANKUMAR B.K., KARIDURAGANOVAR M.Y., Int. J. Current Eng. Technol., **1**, 2013, p. 148.
- URAGAMI T., WAKITA D., MIYATA T., EXPRESS Polym. Lett., **4**, no. 11, 2010, p. 681.
- STOICA-GUZUN A., STROESCU M., JINGA S. I., VOICU G., GRUMEZESCU A.M., HOLBAN A.M., Mater. Sci. Eng., B, **42**, 2014, p. 280.
- KUJAWSKI W., Pol. J. Environ. Stud., **9**, no. 1, 2000, p. 13.
- ZHANG F., ZHANG Y., ZHAO Z., SHEN Z., Chin. J. Polym. Sci., **11**, no. 3, 1993, p. 243.
- DAS S., SARKAR S., BASAK P., ADHIKARI B., J. Sci. Ind. Res., **67**, 2008, p. 219.
- MULDER M.H.V., HENDRICKMAN J.O., HEGEMAN H., SMOLDERS C.A., J. Membr. Sci., **16**, 1983, p. 269.
- CHENG X., LI W., SHAO Z., ZHONG W., YU T., J. Appl. Polym. Sci., **73**, 1999, p. 971

Manuscript received: 2.04.2015